Improve Speed Estimation for Speed-Sensorless Induction Machines: A Variable Adaptation Gain and Feedforward Approach

Lei Zhou, *Member, IEEE* and Yebin Wang, *Senior Member, IEEE*

***Abstract*—This paper investigates speed-sensorless estimation problem for induction machines, aiming to offer a better balance between speed estimation bandwidth and robustness than a classic adaptive full-order observer (AFO). AFO suffers from a trade-off in selecting its speed adaptation gains: large gains for high bandwidth versus low gains for suppression of ripples induced by model mismatches and noises. We propose two revisions on the AFO to relax the trade-off. First is to adopt a variable speed adaptation gain which is large during transient and is small in steady-state. Second is to include a feedforward term in the speed adaptation law to accommodate the rotor's mechanical dynamics. An iterative tuning method is presented to adjust feedforward gains, addressing the uncertainties in rotor's inertia and load torque. Experiments show that the proposed method can significantly improve the speed estimation bandwidth while effectively suppressing the fluctuation of the speed estimate during steady state, compared with AFO.**

***Index Terms*—State Estimation, Motor Drives and Electrical Machines, Induction Machine Drives**

NOMENCLATURE

i_s, u_s	stator current and voltage
Φ_r	rotor flux
ω	rotor angular speed
ω_1	angular speed of the rotating frame
T_L	load torque
J	rotor inertia
R_s, R_r	stator and rotor resistances
L_m, L_s, L_r	mutual, stator, and rotor inductances
σ	$= (L_s L_r - L_m^2)/L_r$
α	$= R_r/L_r$
β	$= L_m/(\sigma L_r)$
γ	$= R_s/\sigma + \alpha\beta L_m$
μ	$= 3L_m/(2L_r)$
$\hat{[\,]}$	denote estimated values
$\tilde{[\,]}$	denote estimation error of values
$[\,]_D, [\,]_Q$	denote quantities in the stationary D-Q frame
$[\,]_d^r, [\,]_q^r$	denote quantities in rotor flux-oriented frame
$\boldsymbol{I}$, $\boldsymbol{J}$	$= \begin{bmatrix} 1 & 0 \\ 0 & 1 \end{bmatrix}, = \begin{bmatrix} 0 & -1 \\ 1 & 0 \end{bmatrix}$

L. Zhou and Y. Wang are with Mitsubishi Electric Research Laboratories, Cambridge, MA 02139, USA (email: {lzhou,yebinwang}@merl.com).

I. INTRODUCTION

For speed sensorless induction motors (IMs) under field-oriented control (FOC), where the motor speed and angular position are not measured, the bandwidth of the speed control is mainly limited by the convergence rate of the state estimation, especially the convergence rate of the speed estimation. Prevailing speed-sensorless IMs suffer significant performance degradation from removing the shaft sensor, which fact limits their applications to fields requiring low or medium dynamic performance. This paper studies improvements toward the classic adaptive full-order observer (AFO) for IMs [1], [2], aiming at increasing the speed estimation bandwidth, and thus enabling the motor being used in circumstances with higher dynamic performance requirements and even servo applications.

Among numerous speed-sensorless estimation methods, the AFO based on the IM fundamental model is still among the most popular and successful estimation methods due to its comprehensive performance including accuracy, robustness, and computational simplicity [3]. However, the classic AFO method often suffers from slow convergence due to the speed adaptation process. In addition, the mechanical dynamics of the rotor are often not included in the estimator, necessarily imposing the assumption that the rotor speed dynamic is slow enough to be treated as a parameter. This assumption significantly simplifies the estimator design and allows the estimation to proceed without knowing the motor's mechanical parameters, but often results in slow speed- estimation transient especially under slow-torque-variation situations [4].

During past years, researchers have been keeping exploring improvements to the AFO regarding its stability and robustness. For example, reference [5] discusses the limitation of the AFO and introduces an alternative design of speed estimator aiming at improving the stability of the estimator, and the proposed speed estimator is applicable for regeneration mode operation. In [6], an AFO design with low frequency signal injection is proposed, which allows the estimator to demonstrate good accuracy and robustness down to zero stator frequency. Reference [7] shows that the classic observer and speed adaptation gain design reveals potential instability in field-weakening region, and proposed an improved gain design method that varies with the speed. Reference [8] studies the parameter sensitivity of sensorless IM with AFO, and proposed a feasible condition for judging

978-1-7281-9945-0/20/$31.00 ©2020 IEEE

the system's stability when there exist model parameter mismatches. An improved AFO design, which does not require the estimated flux error in the speed estimation, is proposed in [9]. In this design, the estimator has guaranteed stability over all speed range and good robustness, however its estimation converges relatively slow. A robust adaptive state observer for IM state and speed estimation is proposed in [10] as a modification to the classic AFO, and its improvements in robustness to model mismatches and disturbances are shown through experiments.

While the aforesaid references mainly concentrate on the estimator's stability and/or its robustness, few study focuses on methods to improve the speed estimation convergence rate of the adaptive estimators. In [11], a set of feedback gains designed by a pole-placement method is proposed. The feedback gains make the speed estimation converge fast theoretically. However, it is demonstrated in practice that the estimation converges very slowly at low speed, mainly due to the sensitivity to parameter mismatch. Reference [12] proposes a feedback gain and adaptation gains using the root-locus method, and has achieved relatively better transient response and tracking accuracy in the speed estimation. However, the design is more complicated, and the speed estimation transient time is about 1 sec, which may be still not fast enough for some highly dynamic applications. In [13], an estimator design that combines the AFO and a sliding mode speed estimation is proposed, and has demonstrated a speed convergence rate of 0.2 sec. This method however, risks introducing large noise in the speed estimation due to the large speed adaptation gain during steady-state operation.

This work aims to improve the speed estimation convergence rate for AFO. Main contributions are listed as follows:

1) Propose a new speed adaptation gain design for the AFO, which can improve the speed estimation convergence rate without sacrificing the noise level in the estimated speed.
2) Propose to add a feedforward term based on the rotor's mechanical dynamics in the speed adaptation law, which further improves the speed estimation bandwidth.
3) Introduce an automatic feedforward gain tuning method based on the iterative tuning method [14], which addresses the difficulty due to the lack of knowledge about the rotor inertia and the load torque.

We have experimentally evaluate the proposed method. Results show that the speed estimation can converge within 0.015 sec under step changes in the command speed, which is about 10 times faster than the baseline AFO.

This paper is organized as follows. Section II provides problem formulation and the AFO as a baseline solution. An improved speed estimation scheme for AFO is proposed in Section IV. Section V shows experimental tests. Conclusion and future work are presented in Section VI.

II. Problem Formulation

Assuming symmetric three-phase excitation and linear magnetic circuit, the IM model in a stator-fixed two-phase D-Q frame is given by

$$\begin{aligned}
\dot{i}_{sD} &= -\gamma i_{sD} + \omega_1 i_{sQ} + \alpha\beta\Phi_{rD} + \beta\Phi_{rQ}\omega + u_{sD}/\sigma, \\
\dot{i}_{sQ} &= -\omega_1 i_{sD} - \gamma i_{sQ} - \beta\Phi_{rD}\omega + \alpha\beta\Phi_{rQ} + u_{sq}/\sigma, \\
\dot{\Phi}_{rD} &= \alpha L_m i_{sD} - \alpha\Phi_{rD} + \omega\Phi_{rQ}, \\
\dot{\Phi}_{rD} &= \alpha L_m i_{sQ} - \omega\Phi_{rD} - \alpha\Phi_{rQ}, \\
\dot{\omega} &= \frac{\mu}{J}(\Phi_{rD} i_{sQ} - i_{sD}\Phi_{rQ}) - \frac{T_L}{J}.
\end{aligned} \tag{1}$$

A rough formulation of the speed sensorless state estimation problem for the IM is: design an estimator to reconstruct the full state of the IM model (1) from measuring stator currents i_{sD}, i_{sQ} and voltages u_{sD}, u_{sQ}.

III. Classic AFO and Performance Discussion

A. Baseline AFO

The classic AFO developed in [1] is introduced for self-containedness. Here, the rotor speed is treated as a slowly time-varying parameter, and the system dynamics in the stationary D-Q frame are

$$\dot{\boldsymbol{x}} = \boldsymbol{A}(\omega)\boldsymbol{x} + \boldsymbol{B}\boldsymbol{u_s}, \quad \boldsymbol{y} = \boldsymbol{C}\boldsymbol{x}. \tag{2}$$

where

$$\boldsymbol{x} = [\boldsymbol{i_s}, \boldsymbol{\Phi_r}]^\top, \qquad \boldsymbol{i_s} = [i_{sD}, i_{sQ}]^\top, \tag{3}$$

$$\boldsymbol{\Phi_r} = [\Phi_{rD}, \Phi_{rQ}]^\top, \quad \boldsymbol{u_s} = [u_{sD}, u_{sQ}]^\top, \tag{4}$$

$$\boldsymbol{A}(\omega) = \begin{bmatrix} -\gamma\boldsymbol{I} & \alpha\beta\boldsymbol{I} - \beta\omega\boldsymbol{J} \\ \alpha L_m\boldsymbol{I} & -\alpha\boldsymbol{I} + \omega\boldsymbol{J} \end{bmatrix}, \tag{5}$$

$$\boldsymbol{B} = \begin{bmatrix} \frac{1}{\sigma}\boldsymbol{I} & \boldsymbol{0} \end{bmatrix}^\top, \boldsymbol{C} = \begin{bmatrix} \boldsymbol{I} & \boldsymbol{0} \end{bmatrix}. \tag{6}$$

With system (2), the following Luenberger observer is employed to estimate the rotor flux

$$\dot{\hat{x}} = \hat{\boldsymbol{A}}\hat{x} + \boldsymbol{B}\boldsymbol{u_s} + \boldsymbol{L}(\boldsymbol{y} - \hat{\boldsymbol{y}}), \quad \hat{\boldsymbol{y}} \ = \boldsymbol{C}\hat{\boldsymbol{x}}, \tag{7}$$

where $\hat{\boldsymbol{A}} = \boldsymbol{A}(\hat{\omega})$, and $\boldsymbol{L}$ is the observer gain matrix. The resultant estimation error dynamics yield

$$\dot{\tilde{\boldsymbol{x}}} = (\boldsymbol{A} - \boldsymbol{L}\boldsymbol{C})\tilde{\boldsymbol{x}} + \Delta\boldsymbol{A}\hat{\boldsymbol{x}}, \tag{8}$$

where

$$\Delta\boldsymbol{A} = \boldsymbol{A} - \hat{\boldsymbol{A}} = \begin{bmatrix} \boldsymbol{0} & -\beta\tilde{\omega}\boldsymbol{J} \\ \boldsymbol{0} & \tilde{\omega}\boldsymbol{J} \end{bmatrix}. \tag{9}$$

A Lyapunov function candidate is selected as

$$V = \tilde{\boldsymbol{x}}^\top\tilde{\boldsymbol{x}} + \tilde{\omega}^2/\lambda, \tag{10}$$

where λ is a positive constant. The time derivative of V is

$$\begin{aligned}
\dot{V} =& \tilde{\boldsymbol{x}}^\top\big((\boldsymbol{A} - \boldsymbol{L}\boldsymbol{C})^\top + (\boldsymbol{A} - \boldsymbol{L}\boldsymbol{C})\big)\tilde{\boldsymbol{x}} \\
&+ 2\tilde{\omega}\beta(\tilde{i}_{sD}\hat{\Phi}_{rQ} - \tilde{i}_{sQ}\hat{\Phi}_{rD}) \\
&+ 2\tilde{\omega}(\tilde{\Phi}_{rQ}\hat{\Phi}_{rD} - \tilde{\Phi}_{rD}\hat{\Phi}_{rQ}) + 2\tilde{\omega}(\dot{\omega} - \dot{\hat{\omega}})/\lambda.
\end{aligned} \tag{11}$$

Assume $\dot{\omega} = 0$, the speed adaptation scheme is selected as

$$\dot{\hat{\omega}} = \lambda\beta(\tilde{i}_{sD}\hat{\Phi}_{rQ} - \tilde{i}_{sQ}\hat{\Phi}_{rD}). \tag{12}$$

Here the flux estimation errors $\tilde{\Phi}_{Dr}$ and $\tilde{\Phi}_{Qr}$ are inaccessible and thus do not appear in (12). Introducing a short notation $e_{i\Phi} = \tilde{i}_{sD}\hat{\Phi}_{rQ} - \tilde{i}_{sQ}\hat{\Phi}_{rD} = \tilde{\boldsymbol{i}}_s \times \hat{\boldsymbol{\Phi}}_r$, the speed adaptation law (12) can be abbreviated as $\dot{\hat{\omega}} = \lambda\beta e_{i\Phi}$.

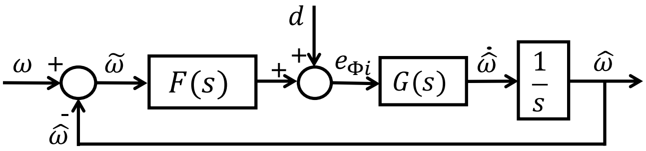

Fig. 1: Speed estimation loop in AFO.

B. Speed Estimation Performance Discussion

This section briefly discusses the performance limitation in the classic AFO via a frequency domain point-of-view. Fig. 1 shows a block diagram of the speed estimation dynamics in the classic AFO for IM. Here, In Fig. 1, $F(s)$ represents the motor and state estimator dynamics of the IM, with the speed estimation error $\tilde{\omega}$ being the input, and the signal $e_{i\Phi}$ being the output. The model parametric errors and steady state estimation error are summarized by an disturbance signal d. The signal $e_{i\Phi}$ goes through an adaptation filter $G(s)$ to generate $\dot{\hat{\omega}}$, and the estimated speed $\hat{\omega}$ can be calculated through integration. According to (12), $G(s)/s = K_{fb}/s$, where $K_{fb} = \lambda\beta$ is a constant. In practice $G(s)/s = (K_p s + K_i)/s$ is typically implemented [1].

The adaptation loop in Fig. 1 shows a fundamental trade-off in the selection of the speed adaptation gain K_{fb}. On one hand, using a large adaptation gain leads to fast speed estimation convergence but can amplify $\tilde{\omega}/d$, which is the sensitivity of the speed estimation error with respect to model parameter mismatch and steady-state flux estimation errors. Such error causes ripple in the estimated speed when the motor is under constant speed operation. On the other hand, using a small adaptation gain yields accurate speed estimation in steady state but has a slow speed estimation convergence. As a result, an adaptation filter with constant gains typically cannot provide satisfactory balance between the conflicting requirements in terms of estimation bandwidth and model uncertainties attenuation.

IV. Proposed Speed Estimation Scheme

This work proposes a novel speed estimation scheme for AFO for IM to better balance the trade-off between estimation bandwidth and disturbance rejection in the speed adaptation. The proposed speed estimation is

$$\dot{\hat{\omega}} = \underbrace{\theta^1(i_{sQ}\hat{\Phi}_{rD} - i_{sD}\hat{\Phi}_{rQ}) - \theta^2}_{\text{feedforward term}} + \underbrace{k_{fb}(e_{i\Phi})e_{i\Phi}}_{\text{feedback term}}, \tag{13}$$

where θ^1 and θ^2 are the feedforward gains, and k_{fb} is the feedback gain. Particularly, k_{fb} is a function of the signal $e_{i\Phi}$. The design of the two terms are discussed in detail as follows.

A. Nonlinear Feedback Speed Adaptation Gain

The feedback term in the speed estimation (13) include a variable feedback gain k_{fb} to address the trade-off between (i) the requirement of using a high adaptation gain during transient for speed estimation convergence rate improvement, and (ii) the requirement of using a small adaptation gain during steady-state operation for mitigating the oscillation and inaccuracy in the estimated speed.

In AFO for IM, the signal $e_{i\Phi}$ contains information of the motor operation mode. When the motor is in steady-state running, $e_{i\Phi}$ demonstrates a periodic oscillation of small amplitude, and the fundamental frequency of this periodic oscillation is the frequency of the motor. This speed ripple is induced by the disturbance signal d, which includes the model parametric error and steady-state estimation errors in currents and fluxes. During motor speed transient, e.g., when the motor is accelerating or decelerating, the signal $e_{i\Phi}$ presents a relatively large magnitude, and will converge to its steady-state value after the transient.

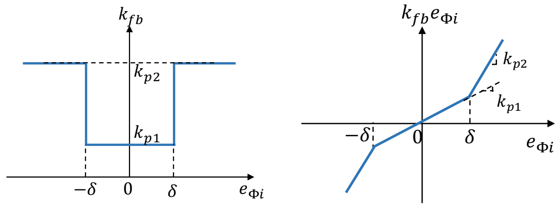

Fig. 2: Left: Switching-type variable feedback gain. Right: feedback term.

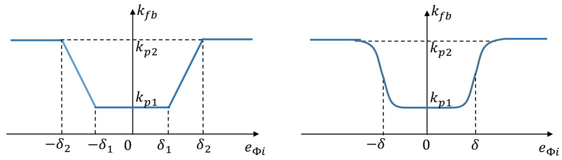

Fig. 3: Other possible feedback adaptation gain selections. Left: linear transition adaptation gain. Right: sigmoid transition adaptation gain.

Based on the aforesaid observations, the feedback gain k_{fb} in (13) is designed as a function of $e_{i\Phi}$. The feedback gain k_{fb} should demonstrate a small amplitude when $e_{i\Phi}$ is around its typical steady-state magnitude, and has a large amplitude when $e_{i\Phi}$ is around its typical value during transient. Many possible selections for the speed adaptation gain that has these characteristics can be used. For example, k_{fb} may be selected as the following switching form:

$$k_{fb} = \begin{cases} k_{p1} & \text{if } -\delta \le e_{i\Phi} \le \delta, \\ k_{p2} & \text{if } e_{i\Phi} > \delta \text{ or } e_{i\Phi} < -\delta, \end{cases} \tag{14}$$

where k_{p1}, k_{p2} are positive constants and $k_{p1} < k_{p2}$, and δ is a constant that sets the adaptation gain switching threshold. Fig. 2 shows the feedback gain k_{fb} and the feedback term $k_{fb}e_{i\Phi}$ of (14). Alternatively, k_{fb} can be selected as

$$k_{fb} = \min\big(\max(k_{p1}, a_1 + a_2|e_{i\Phi}|), k_{p2}\big), \tag{15}$$

where a_1, a_2 are positive constants that set the linear gain switching between k_{p1} and k_{p2}. Similarly, k_{fb} can be chosen as the following smooth switching form

$$k_{fb} = k_{p1} + (k_{p2} - k_{p1})\max\big(s(e_{i\Phi} - \delta), 1 - s(e_{i\Phi} + \delta)\big), \tag{16}$$

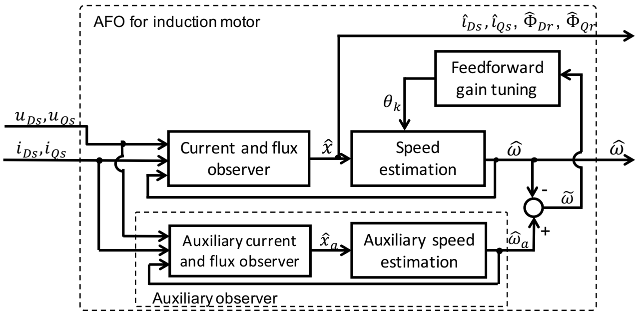

Fig. 4: Block diagram of the feedforward gain tuning in IM state observer.

where $s(x) = 1/(1+\exp(-x))$ is the sigmoid function. Fig. 3 shows the example feedback gains given in (15) and (16).

B. Feedforward Speed Estimation

The objective of adding the feedforward term in (13) is to ensure that the speed estimation matches the rotor dynamics. Comparing the rotor dynamics in (1) and the speed estimator (13), it can be seen that if the feedforward gains are selected as $\theta^1 = \mu/J$ and $\theta^2 = T_L/J$, the feedforward term will enable the estimated speed $\hat{\omega}$ to track the true rotor speed ω under the condition that the flux estimation has converged.

The inclusion of the feedforward term in the speed adaptation law can also be derived through substituting an estimate for the rotor speed dynamics $\dot{\omega} = \mu(i_{Qs}\hat{\Phi}_{Dr} - i_{Ds}\hat{\Phi}_{Qr})/J - T_L/J$ into (11), which implies that instead of regarding the rotor speed as a constant parameter, the speed is treated as a time-varying parameter with known dynamics.

The feedforward term significantly improves the transient performance of the speed estimation. However, in practice, motor's mechanical parameters, such as the rotor inertia and the load torque, are often not exactly known. Besides, the load torque could be time-varying, which adds further challenge in the tuning of the feedforward gains. In this work, an iterative tuning method is used to tune the feedforward gains automatically. The iterative tuning method has been used to fine-tune controllers in a repetitive process using only data collected in experiment runs. In this method, the controller parameters are chosen to minimize a certain cost function, and the values of the control parameters are updated iteratively with a gradient search [14]. The algorithm has been used in the feedforward controller tuning for precision motion systems such as linear motors and wafer stages [15]–[17].

The feedforward gain tuning using the iterative tuning method is through the optimization of a certain objective function, which represents the performance of the speed estimator. In the case that the motor speed could be directly measured, the objective function could be selected as $J(\boldsymbol{\theta}) = \tilde{\omega}^\top\tilde{\omega}$, where $\boldsymbol{\theta} = [\theta^1, \theta^2]^\top$. In the speed sensorless circumstance, the motor speed is not available for direct measurement. In this design, the speed estimation from an auxiliary estimator is selected as a ground truth signal, and the error between the two speed estimations is used in the cost function for tuning the feedforward gains. Define an auxiliary state estimate $\hat{\boldsymbol{x}}_a = [i^a_{sD}, i^a_{sQ}, \Phi^a_{rD}, \Phi^a_{rQ}]^\top$ and an auxiliary speed estimate $\hat{\omega}_a$. The auxiliary estimator consists of a state observer as follows

$$\dot{\hat{\boldsymbol{x}}}^a = \hat{\boldsymbol{A}}\hat{\boldsymbol{x}} + \boldsymbol{B}\boldsymbol{u}_s + \boldsymbol{L}(\boldsymbol{y} - \boldsymbol{C}\hat{\boldsymbol{x}}^a), \tag{17}$$

which is in the same form with (7). The auxiliary estimator employs the following speed adaptation law

$$\dot{\hat{\omega}}_a = k_{fb}(e^a_{\Phi i})e^a_{\Phi i}, \tag{18}$$

where $e^a_{\Phi i} = \tilde{i}^a_{sD}\hat{\Phi}^a_{rQ} - \tilde{i}^a_{sQ}\hat{\Phi}^a_{rD}$. Eq. (18) is in the same form with (13) except that the feedforward term is not included, which ensures $\hat{\omega}^a$ does not demonstrate steady-state speed estimation errors due to feedforward. Using the auxiliary estimated speed $\hat{\omega}_a$ as an reference signal in the tuning of the feedforward term, the optimization problem for feedforward estimation gain tuning can be formulated as

$$\min_{\boldsymbol{\theta}} \; J(\boldsymbol{\theta}) = (\hat{\omega}_a - \hat{\omega})^2. \tag{19}$$

It is assumed that no constraint is present on the selection of the feedforward gains, i.e., the optimization problem (19) is unconstrained. Since $\hat{\omega}_a - \hat{\omega}$ is a linear function of θ, problem (19) is convex, and its the global optimal solution can be solved reliably. The values of the feedforward gains can be updated iteratively using a gradient-based search as

$$\dot{\boldsymbol{\theta}} = -\alpha\boldsymbol{R}^{-1}\frac{\partial J(\boldsymbol{\theta})}{\partial\boldsymbol{\theta}}, \tag{20}$$

where α is the step size, $\boldsymbol{R}$ is a matrix to modify the search direction, and $\frac{\partial J}{\partial\boldsymbol{\theta}}$ is the gradient evaluated at $\boldsymbol{\theta}$.

C. Tuning Method

This section briefly discusses the tuning for the proposed speed estimation scheme.

1) Feedback Gain Tuning: Parameters for the nonlinear feedback gain (14) include: (i) steady-state gain k_{p1}, (ii) the transient-time gain k_{p2}, and (iii) the switching threshold δ. The values of these parameters can be determined as follows. Assume the maximum acceptable speed ripple magnitude is δ_r. The steady-state gain k_{p1} can be selected as the largest gain such that the speed ripple of magnitude smaller than δ_r. The value of δ can be selected as δ_r times with an additional margin.

There are two methods to determine the value of k_{p2}. If a shaft sensor is used during the tuning process, the value of k_{p2} can be directly determined by the measured speed estimation dynamic performance, for example the rise time of the estimated speed. If the motor does not have speed measurement during tuning, k_{p2} can be selected via analysis for the speed adaptation loop shown in Fig. 1. Given a target speed estimation convergence rate, the target cross-over frequency of the speed adaption loop can be found, and the required k_{p2} value can then be calculated.

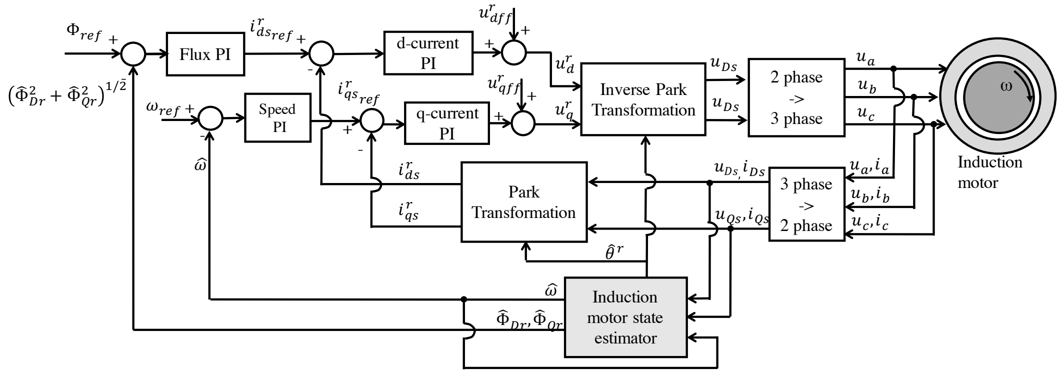

Fig. 5: Block diagram of the FOC with estimated speed and flux being used for feedback.

TABLE I: Parameters of IM model.

Parameter	Value
Stator resistance R_s	11.05Ω
Rotor resistance R_r	2.133Ω
Stator self-inductance L_s	0.23 H
Rotor self-inductance L_r	0.23 H
Mutual Inductance L_m	0.22 H
Rotor inertia J	0.0012 kgm^2
Number of pole pairs p	2
Motor power	180 W

2) Feedforward Gain Tuning: The feedforward estimation gains are tuned by the iterative tuning method either online or offline. For offline tuning, the system in Fig. 4 can be used to identify the required feedforward gains at varying speeds, and the identified feedforward gains are stored in a loop-up table. When the motor is operating, the speed estimator retrieves the stored feedforward gain values. This method can avoid the gain-tuning dynamics when the motor is operating and results in a faster speed transient, however it requires the working condition of the IM being fixed and known.

The online feedforward gain tuning method implements the iterative tuning system in Fig. 4 when the motor is operating, and the system identifies the appropriate feedforward gains in real-time. This method can be used when the motor is driving a variable load. However the tuning dynamics may impair the speed estimation bandwidth especially under varying load condition, and the tuning dynamics need to be designed carefully. Typically the feedforward gain tuning convergence rate is selected to be 10 times slower than that of the speed estimation to ensure stability.

V. Experimental Evaluation

The proposed state estimation method was experimentally tested with a Marathon™ three-phase IM. Control algorithm was compiled by Matlab/Simulink™, and downloaded to dSPACE™ DS1104 for realtime operation. A PWM inverter was used to energize the motor. The control loop ran at a sampling frequency of 4 kHz, and the PWM frequency was also 4 kHz. Parameters of the IM are shown in Table I.

The tracking controller implements a standard indirect FOC as is shown in Fig. 5. Four PI controllers were used to regulate speed, rotor flux amplitude, and stator currents in d- and q-axis, respectively. Table II shows the value of the controller parameters tuned by trail and error. The rotor flux magnitude estimate was achieved by $\hat{\Phi}_r = (\hat{\Phi}_{Dr}^2 + \hat{\Phi}_{Qr}^2)^{1/2}$. In Fig. 5, the feedforward control signals are $u_{dff}^r = -\sigma\omega_e i_{qs}$, $u_{qff}^r = \sigma(\omega_e i_{ds} + \beta\hat{\omega}\hat{\Phi}_{dr}^r)$. The field angle estimate is computed by $\dot{\hat{\theta}} = \hat{\omega} + \alpha L_m i_{qsref}^r/\Phi_{ref}$.

TABLE II: PI Controller Parameters.

Controller	K_p	K_i
Flux PI	5	0.1
Speed PI	10	0.1
d-current PI	20	0.2
d-current PI	20	0.2

A. Open-loop Speed Estimation without Feedforward

The proposed state estimator was first tested in open-loop, where the motor speed measured with an optical encoder was used for feedback. This experiment provides a fair comparison between different estimation schemes. The speed estimation performance of AFO with a variable speed adaptation gain was tested and compared with baseline AFO with a constant speed adaptation gain. The feedforward speed estimation term was not included. In our implementation, a step-type variable speed estimation gain, as is shown in (14) and Fig. 2, was being used with $k_{p1} = 5 \times 10^3$ and $k_{p2} = 5 \times 10^4$. In the speed estimator with constant speed adaptation gain, the adaptation gain was selected as $k_p = 5 \times 10^3$. Both estimators use an identical flux observer.

Fig. 6 shows the speed estimation performance comparison between the variable gain and constant gain speed estimation. Both estimators can stably estimate the speed. The variable gain speed estimator shows a significantly faster speed estimation convergence rate, which is due to the high adaptation gain during the transient. During steady-state operation, the two estimators show similar speed ripple amplitude. This is because both estimators share the same speed adaptation gain. Note that the variable gain estimated speed demonstrates an under-shoot at the beginning of the speed step response. This is also a consequence of the large feedback gain in the speed adaptation law and a relatively large current estimation error $\tilde{i}_{qs}$ in transient.

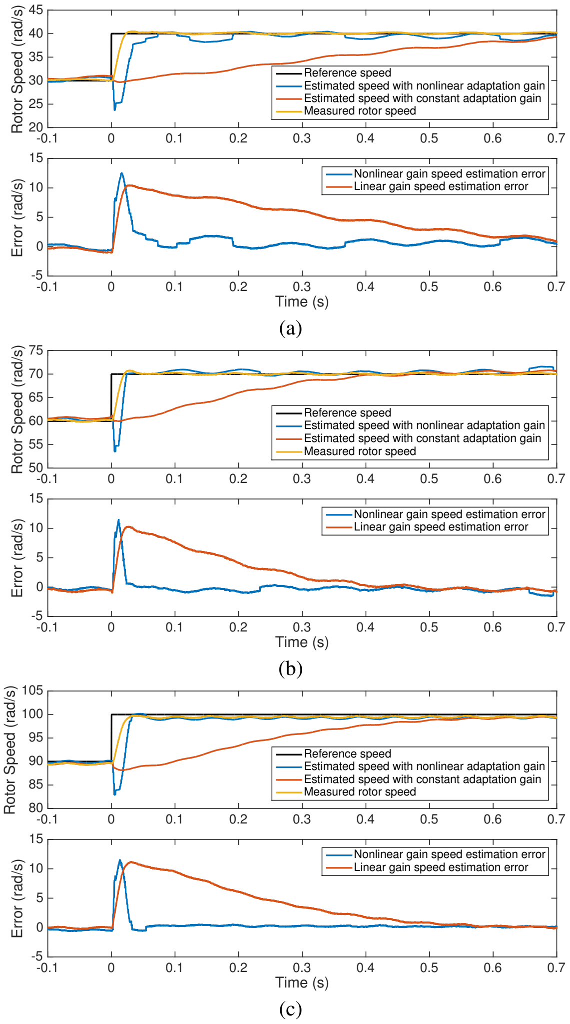

Fig. 6: Comparison between nonlinear speed estimation gain and constant speed estimation gain under step-type speed reference. Feedforward speed estimation is not included. (a) 30-40 rad/s. (b) 60-70 rad/s. (c) 90-100 rad/s.

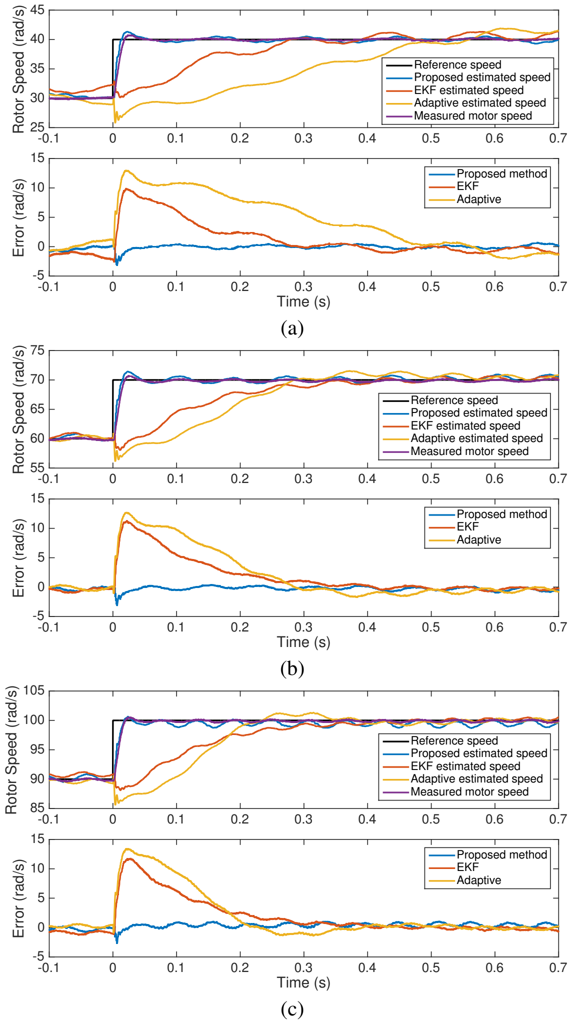

Fig. 7: Comparison between baseline AFO, EKF, and the proposed speed estimation method under step-type speed reference. (a) 30-40 rad/s. (b) 60-70 rad/s. (c) 90-100 rad/s.

B. *Open-loop Speed Estimation with Feedforward*

The proposed estimation method with the feedforward term included was tested and compared with the speed estimation performance of the the baseline adaptive flux observer and the extended Kalman filter (EKF) method, as is shown in Fig. 7. Again, the measured speed was used for feedback, and the observers ran in open-loop. The data were taken after the feedforward gain auto-tuning has converged. Among the three estimators, the proposed method has the fastest speed estimation convergence rate: the speed estimation transient of the proposed method converges within 0.015 s, while the baseline EKF and adaptive methods take about 0.3 s to converge. As shown in the speed estimation error plots, the speed estimation error of the proposed method is shooting downwards during transient. This implies that the estimated speed is leading the true motor speed due to the feedforward speed estimation.

C. *Closed-loop Speed Estimation and Control*

Finally the proposed estimator was tested in closed-loop, where the estimated speed was used for feedback control. Fig. 8 shows the estimated and measured speed data. In this experiment, the IM speed step response demonstrates a rise time of 0.02 s under different operating speeds. In comparison, using the estimated speed from the baseline AFO and the EKF method require reducing the speed control gain to maintain stability. This experiment shows that the proposed method can effectively increase the closed-loop speed control bandwidth of the sensorless IMs.

VI. Conclusion

In this paper, a new speed estimation method in AFO for IM was proposed and tested. The proposed speed estimation method uses a combination of feedforward and feedback. The feedforward gains can be automatically tuned using an iterative tuning method, and the feedback gain is designed to be nonlinear to better balance the trade-off between the

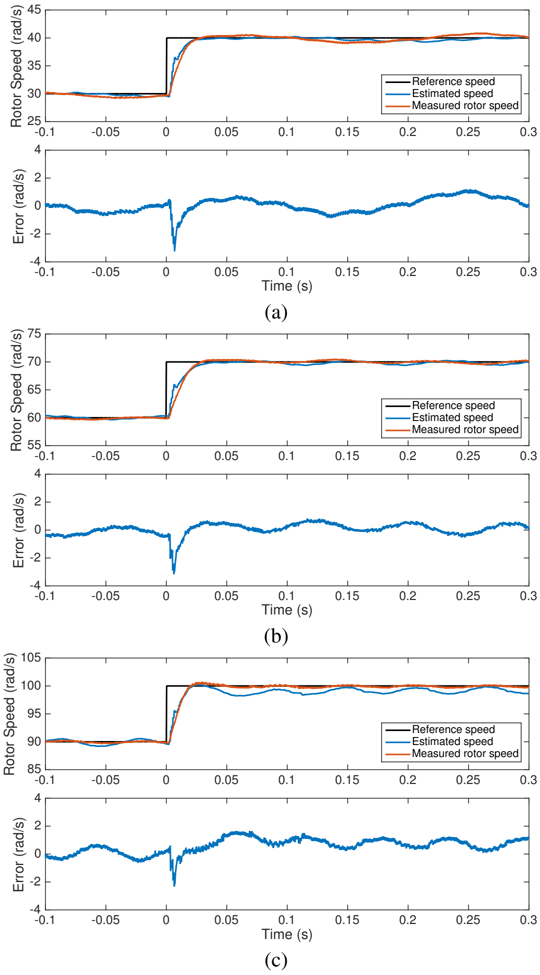

Fig. 8: Measured and estimated speed under step-type speed reference with the estimated speed being used for control. (a) 30-40 rad/s. (b) 60-70 rad/s. (c) 90-100 rad/s.

high bandwidth and low noise requirements. Tuning of the proposed method was discussed. Experimental results demonstrate that the proposed method can effectively improve the speed estimation convergence rate without amplifying the speed ripple in steady-state operation, and a 0.02 s rise time in the speed step response can be achieved for a sensorless IM with the proposed speed estimation method.

References

[1] H. Kubota, K. Matsuse, and T. Nakano, "Dsp-based speed adaptive flux observer of induction motor," *IEEE Trans. Ind. Appl.*, vol. 29, no. 2, pp. 344–348, 1993.

[2] H. Kubota and K. Matsuse, "Speed sensorless field-oriented control of induction motor with rotor resistance adaptation," *IEEE Trans. Ind. Appl.*, vol. 30, no. 5, pp. 1219–1224, 1994.

[3] J. Holtz, "Sensorless control of induction machines-with or without signal injection?" *IEEE Transactions on Industrial Electronics*, vol. 53, no. 1, pp. 7–30, 2006.

[4] M. Barut, S. Bogosyan, and M. Gokasan, "Speed-sensorless estimation for induction motors using extended kalman filters," *IEEE Trans. Ind. Electron.*, vol. 54, no. 1, pp. 272–280, 2007.

[5] H. Tajima, G. Guidi, and H. Umida, "Consideration about problems and solutions of speed estimation method and parameter tuning for speed-sensorless vector control of induction motor drives," *IEEE Trans. Ind. Appl.*, vol. 38, no. 5, pp. 1282–1289, 2002.

[6] M. Hinkkanen, V.-M. LEPPÄNEN, and J. LUOMI, "Flux observer enhanced with low-frequency signal injection allowing sensorless zero-frequency operation of induction motors," *IEEE Trans. Ind. Appl.*, vol. 41, no. 1, pp. 52–59, 2005.

[7] M. Hinkkanen, "Analysis and design of full-order flux observers for sensorless induction motors," *IEEE Trans. Ind. Electron.*, vol. 51, no. 5, pp. 1033–1040, 2004.

[8] B. Chen, W. Yao, F. Chen, and Z. Lu, "Parameter sensitivity in sensorless induction motor drives with the adaptive full-order observer," *IEEE Trans. Ind. Electron.*, vol. 62, no. 7, pp. 4307–4318, 2015.

[9] W. Sun, Y. Yu, G. Wang, B. Li, and D. Xu, "Design method of adaptive full order observer with or without estimated flux error in speed estimation algorithm," *IEEE Trans. Power Electron.*, vol. 31, no. 3, pp. 2609–2626, 2016.

[10] Z. Yin, Y. Zhang, C. Du, J. Liu, X. Sun, and Y. Zhong, "Research on anti-error performance of speed and flux estimation for induction motors based on robust adaptive state observer," *IEEE Transactions on Industrial Electronics*, vol. 63, no. 6, pp. 3499–3510, 2016.

[11] S. Sangwongwanich, S. Suwankawin, and S. Koonlaboon, "A unified speed estimation design framework for sensorless ac motor drives based on positive-real property," in *Power Conversion Conference-Nagoya, 2007. PCC'07.* IEEE, 2007, pp. 1111–1118.

[12] B. Chen, T. Wang, W. Yao, K. Lee, and Z. Lu, "Speed convergence rate-based feedback gains design of adaptive full-order observer in sensorless induction motor drives," *IET Electric Power Applications*, vol. 8, no. 1, pp. 13–22, 2014.

[13] J. Li, A. Thapa, and K. A. Corzine, "Speed-sensorless drive for induction machines using a novel hybrid observer," in *Applied Power Electronics Conference and Exposition (APEC), 2017 IEEE.* IEEE, 2017, pp. 512–517.

[14] H. Hjalmarsson, M. Gevers, S. Gunnarsson, and O. Lequin, "Iterative feedback tuning: theory and applications," *Control Systems, IEEE*, vol. 18, no. 4, pp. 26–41, 1998.

[15] H. Stearns, S. Mishra, and M. Tomizuka, "Iterative tuning of feedforward controller with force ripple compensation for wafer stage," in *Advanced Motion Control, 2008. AMC'08. 10th IEEE International Workshop on.* IEEE, 2008, pp. 234–239.

[16] M. Heertjes, D. Hennekens, and M. Steinbuch, "Mimo feed-forward design in wafer scanners using a gradient approximation-based algorithm," *Control Engineering Practice*, vol. 18, no. 5, pp. 495–506, 2010.

[17] B. Van der Velden, T. Oomen, and M. F. Heertjes, "Constrained iterative feedback tuning for robust high-precision motion control," in *IFAC World Congress*, 2014, pp. 1–6.

VII. Biographies

Lei Zhou (M'20) received the B.S. degree from the Department of Precision Instrument and Mechanology, Tsinghua University, China, in 2012, and received S.M., and Ph.D. degree from the Department of Mechanical Engineering at Massachusetts Institute of Technology in 2014 and 2019. She is a Visiting Research Scientist with Mitsubishi Electric Research Laboratories in Cambridge, MA, USA since 2019. Her research interests include control, estimation and precision mechatronics.

Yebin Wang (M'09-SM'16) received the B.Eng. degree in Mechatronics Engineering from Zhejiang University, China, in 1997, M.Eng. degree in Control Theory & Control Engineering from Tsinghua University, China, in 2001, and Ph.D. in Electrical Engineering from the University of Alberta, Canada, in 2008. Dr. Wang has been with Mitsubishi Electric Research Laboratories in Cambridge, MA, USA, since 2009, and now is a Senior Principal Research Scientist. From 2001 to 2003 he was a Software Engineer, Project Manager, and Manager of R&D Dept. in automation industries, Beijing, China. His research interests include nonlinear control and estimation, optimal control, adaptive systems and their applications including mechatronic systems.